World Journal of Advanced Research and Reviews
eISSN: 2581-9615 CODEN (USA): WJARAI
Cross Ref DOI: 10.30574/wjarr
Journal homepage: https://wjarr.com/

(RESEARCH ARTICLE)

Check for updates

# Assessment of Differences in Liquefaction Potential Using Standard Penetration Test and Shear-Wave Velocity Data Obtained at 10 Sites in West Tennessee

Hamed Tohidi [1,*], David Arellano [2] and Shahram Pezeshk [2]

[1] *Dam Safety Group, Seattle City Light, Seattle, WA, 98104.*
[2] *Department of Civil, Construction, and Environmental Engineering, The University of Memphis, Memphis, TN, 38152.*

World Journal of Advanced Research and Reviews, 2025, 28(01), 058-067

Publication history: Received on 21 August 2025; revised on 27 September 2025; accepted on 30 September 2025

Article DOI: https://doi.org/10.30574/wjarr.2025.28.1.3376

## Abstract

This paper compares the liquefaction potential at 10 West Tennessee sites using two sets of field test data. The liquefaction potential at each test site is estimated using Standard Penetration Test (SPT) and Shear-wave Velocity (Vs) measurements. Liquefaction Potential Index (LPI) is determined at each site, and comparisons are made between LPIs obtained using SPT and the Vs data. For most of the sites, LPIs based on Vs data are higher than the LPIs obtained using SPT N-values at the same location. The primary reasons for the differences in LPIs are the variation of empirical relationships for estimating cyclic resistance ratio (CRR), which is different between SPT and the Vs, and the impact of the weighting function of the LPI equation. CRR is mainly a function of $(N_1)_{60CS}$ and $Vs_1$ values with depth for the SPT and Vs methods, respectively. The weighting function is dependent on the depth of the liquefiable layer. A comparison is made between the number and depth of liquefiable layers of SPT and Vs methods at each site. The number and depth of liquefiable layers are the primary reasons for differences in CRR and the weighting function impact; consequently, LPI.

**Keywords:** Liquefaction; LPI; SPT; Shear wave velocity; New Madrid seismic zone

## 1. Introduction

Soil liquefaction is one of the most catastrophic earthquake consequences in which loose saturated soils lose shear strength due to the dynamic loading of an earthquake. Since 1964 and after the disastrous Niigata and Alaska earthquakes, several researchers studied liquefaction e.g., [1-8]. One of the most common methods of liquefaction analyses is the simplified method developed by Seed and Idriss [1], which has been updated and modified over the last five decades. Researchers and engineers use the simplified procedure all around the world. The simplified procedure was initially based on the Standard Penetration Test (SPT) (i.e., SPT N-values). Since 1971, the simplified procedure has been extended to include Cone Penetration Test (CPT), Becker Penetration Test (BPT), Dilatometer Testing (DMT), and Shear Wave Velocity ($V_s$) measurements. Various researchers have compared the results of the liquefaction potential evaluation using the simplified method based on various in-situ tests [9-18]. The results of these studies indicate that the liquefaction potential outcomes between the SPT N-value and the shear wave velocity ($V_s$) measurements generally do not agree, and there is no consensus on which field test method provides a more accurate or conservative outcome. Most of these studies do not compare liquefaction potential from different field tests obtained from the same locations. Verdugo [19] argued that the shear wave velocity has some limitations in predicting the liquefaction potential. He concluded that the correlation between $V_s$ and the liquefaction resistance is weak because of the insensitivity of $V_s$ to parameters such as the over-consolidation ratio, which significantly impacts the liquefaction resistance. Additionally, this study compares the liquefaction potential between SPT and $V_s$ field test results obtained at the same location at 10 sites in West Tennessee.

* Corresponding author: Hamed Tohidi

## 2. Material and Methods

### 2.1. Field Test Data

This study utilizes SPT and $V_s$ data obtained from downhole seismic surveys by Pezeshk et al. [20] at 10 sites located in West Tennessee. Table 1 provides the locations of the 10 sites. The 200-ft deep boreholes at Route 14, Sommerville, Covington, Brownsville, Newbern, and Trenton, Tennessee, were drilled in Quaternary Loess that was underlain by tertiary deltaic-marine deposits. The 200-ft borehole at Wynnburg was drilled in Quaternary Alluvial deposits, and the 104-ft borehole at Selmer was drilled in Cretaceous McNairy sand. Jackson and Paris sites were drilled to depths of 200 ft and 100 ft deep, respectively, within the Tertiary Jackson Formation which is underlain by Tertiary Poters Creek clay and Clayton Formation [20]. The site locations and general description of geology are shown in Fig. 1. Shear wave velocity and SPT profiles are provided in Pezeshk et al. [20].

**Table 1** Locations of the SPT and $V_s$ data used in this study [20]

| Site | Latitude | Longitude |
|---|---|---|
| Route 14 | 35°18.53′ | 89°49.41′ |
| Sommerville | 35°16.74′ | 89°21.54′ |
| Covington | 35°24.02′ | 89°37.50′ |
| Brownsville | 35°32.34′ | 89°15.60′ |
| Newbern | 35°08.28′ | 89°14.88′ |
| Jackson | 35°38.11′ | 88°55.20′ |
| Selmer | 35°10.50′ | 88°36.24′ |
| Trenton | 35°57.93′ | 88°56.83′ |
| Paris | 36°16.03′ | 88°20.18′ |
| Wynnburg | 36°19.27′ | 89°28.48′ |

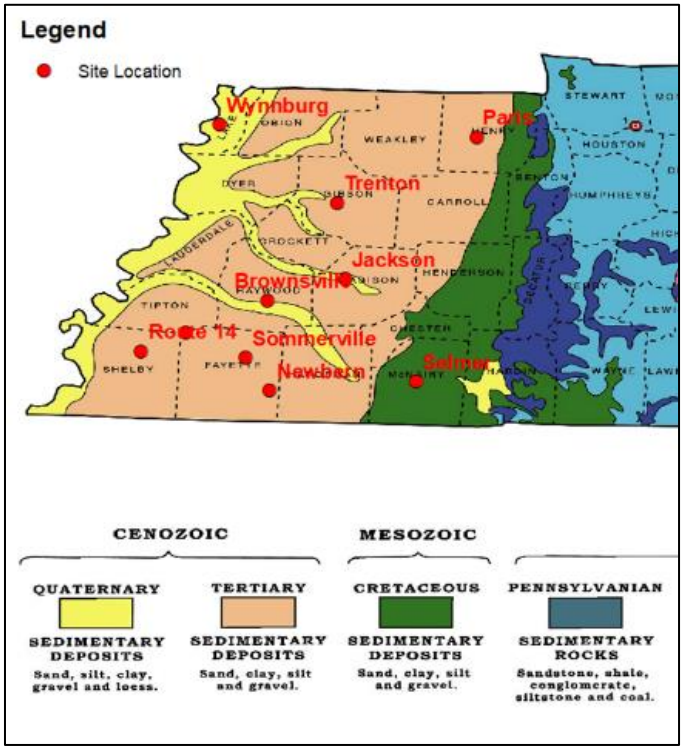


**Figure 1** Study area with geology background and the location of investigated sites

### 2.2. Liquefaction potential analysis

For this study, the liquefaction potential at a given location is based on the Liquefaction Potential Index (LPI) method [3,4]. Many researchers use the LPI method to assess the liquefaction potential in North America [21-24]. The LPI is obtained by:

$$LPI = \int_0^{20} F(z) \cdot w(z) \cdot dz \quad (1)$$

where $z$ is the depth (0 to 20 m), $w(z)$ is the weighting function, which is equal to 10 - 0.5$z$, $dz$ is the differential increment of depth, and $F$(z) is the severity, which is a function of the factor of safety (FS) and it is computed by:

$$\begin{cases} F(z)=1-FS & \text{for } 0 \le \text{FS} \le 1, \\ F(z)=0 & \text{for FS} > 1 \end{cases} \quad (2)$$

The weighting function decreases with an increase in depth in the LPI procedure, and it is one of the primary reasons for the difference in the LPI values between the SPT and $V_s$ methods because the liquefiable layers depth varies in each method which will be discussed later in this article.

The parameter FS is based on the simplified procedure [1] and is determined at a given depth in a soil profile using the following equation:

$$FS = \frac{CRR}{CSR} \cdot MSF.K_\sigma.K_\alpha \quad (3)$$

where CRR is the cyclic resistance ratio, which is the capacity of soil to resist liquefaction, and CSR is the cyclic stress ratio and represents the exerted dynamic stress induced by an earthquake on the soil. MSF is a magnitude scaling factor that corrects for magnitudes other than 7.5. MSF is determined to be 1 for a moment magnitude ($M_w$) of 7.5 and is used in this study, $K_\alpha$ is a correction factor for the sloping ground which is considered 1 in this study, and $K_\sigma$ is an overburden correction factor for soil layers with overburden pressure > 100 kpa, and is computed using:

$$K_\sigma = \left(\frac{\sigma'_{v0}}{P_a}\right)^{f-1} \quad (4)$$

where $\sigma'_{v0}$ is vertical effective overburden stress; $P_a$ is the atmospheric pressure and is equal to 100 kpa, and $f$ is an exponent function that ranges between 0.6 to 0.8. CSR is given by:

$$CSR = 0.65\left(\frac{a_{max}}{g}\right)\left(\frac{\sigma_v}{\sigma'_v}\right)r_d \quad (5)$$

where $a_{max}$ is the peak ground acceleration, g is the acceleration of gravity (9.8 m/sec$^2$), $\sigma_v$ is the total vertical stress, and $r_d$ is the stress reduction coefficient and is computed using a revised equation suggested by Idriss [25] as the following:

$$r_d = \exp\left[\alpha(z) + \beta(z)M_W\right] \quad (6)$$

where,

$$\begin{cases} \alpha(z) = -1.012 - 1.12\sin\left(\frac{z}{11.7} + 5.133\right) \\ \beta(z) = 0.106 + 0.118\sin\left(\frac{z}{11.3} + 5.142\right). \end{cases} \quad (7)$$

One primary difference in evaluating the liquefaction potential using the LPI method and the simplified methods between SPT and $V_s$ data is in determining CRR. Both SPT and $V_s$-based CRR procedures were utilized from the approved equations of the 1996 NCEER and 1998 NCEER/NSF Workshops [7]. The SPT-based CRR is given by:

$$CRR_{7.5} = \left(\frac{1}{34-(N_1)_{60CS}} + \frac{(N_1)_{60CS}}{135} + \frac{50}{(10((N_1)_{60CS})+45)^2} - \frac{1}{200}\right) \quad (8)$$

where $(N_1)_{60CS}$ is the corrected N-value for clean sand and is given by:

$$(N_1)_{60CS} = \alpha + \beta((N_1)_{60}) \quad (9)$$

where $\alpha$ and $\beta$ are functions of fines content (FC) and are estimated as:

$$\begin{cases} \alpha = 0 & FC \leq 5\ \% \\ \alpha = \exp\left[1.76 - \left(\frac{190}{FC^2}\right)\right] & 5\% < FC < 35\ \% \\ \alpha = 1.2 & FC \geq 35\% \\ \text{and} & \\ \beta = 1.0 & FC \leq 5\ \% \\ \beta = \left[0.99 + \left(\frac{FC^{1.5}}{1000}\right)\right] & 5\% < FC < 35\ \% \\ \beta = 5 & FC \geq 35\% \end{cases} \quad (10)$$

Note that for FC ≤5, $(N_1)_{60CS} = (N_1)_{60}$ where $(N_1)_{60}$ is the corrected SPT N-value of field and is calculated by:

$$(N_1)_{60} = N \cdot C_N \cdot C_E \cdot C_B \cdot C_R \cdot C_S \quad (11)$$

where $N$ is the measured standard penetration resistance, $C_N$ is the overburden correction factor and is computed by $\left(\frac{P_a}{\sigma'_{v0}}\right)^{0.5}$, $C_E$ is the hammer energy ratio correction factor, $C_B$ is the borehole diameter correction factor, $C_R$ is the rod length correction factor, and $C_S$ is the correction factor for samplers with or without liners.

The SPT-based $CRR_{7.5}$ in equation 8 was provided by Youd and Idriss [7]. This relationship is valid for $(N_1)_{60CS} < 30$ because it is assumed that for $(N_1)_{60CS} \geq 30$, the soils are too dense to liquefy; therefore, it can be concluded that soil layers with N-values of 30 or higher are non-liquefiable [7]. The CRR procedure based on $V_s$ data [26] is given by:

$$CRR_{7.5} = \left\{\left(0.022\frac{V_{s1}}{100}\right) + 2.8\left(\frac{1}{c - V_{s1}} - \frac{1}{c}\right)\right\} \quad (12)$$

where $V_{s1}$ is the corrected shear wave velocity for the effective overburden stress and is given by $V_{s1} = V_s\left(\frac{P_a}{\sigma'_{v0}}\right)^{0.25}$, $c$ is a function of FC and is determined based on the FC for a soil layer given by:

$$\begin{cases} c = 215\ \text{m/s} & FC \leq 5\% \\ c = 215 - 0.5(FC - 5)\ \text{m/s} & 5\% < FC < 35\% \\ c = 200\ \text{m/s} & FC \geq 35\% \end{cases} \quad (13)$$

The $V_s$-based CRR equation was developed by Andrus and Stokoe [26]. In the $V_s$ approach, the $V_{s1}$ value of 210 m/s was considered the upper limit value [26]. Soil layers with $V_{s1}$ higher than 210m/s are deemed to be non-liquefiable [7]. In other words, the $V_{s1}$ value of 210m/s is considered equivalent to the $(N_1)_{60}$ of 30 for clean sand.

SPT boring logs and $V_s$ profiles of all 10 sites were utilized for this study. The boring logs included SPT N-values at various depths. The $V_s$ values were measured at the boring logs at all 10 sites using downhole seismic surveys.

The reported groundwater level (GWL) for all 10 sites by Pezeshk et al. [20] was used in this study. Therefore, the same unit weights of soil layers with depth and the same GWLs for both SPT and $V_s$ methods at each site were used. Thus, the CSR with depth is the same for SPT and $V_s$ methods at a given site.

In both CRR equations of SPT (equation 8) and $V_s$ (equation 12) methods of liquefaction potential evaluation, there is/are one or more parameters involved that are estimated based on the FC of soil layers. The FC of each soil layer of SPT borings and $V_s$ profiles in this study was approximated using the study by Rix and Romero-Hudock [27], which is based on the Unified Soil Classification System (USCS). Because the location of $V_s$ profiles and SPT borings at each site was the same, the equal amount of FC was considered for both $V_s$ and SPT profiles at each site. This eliminates the variability of FC. Also, it is reasonable that the SPT and $V_s$ profiles of each site have the same soil layers since their location is the same.

In summary, CRR and the weighting function of the LPI are the primary differences between evaluating the liquefaction potential using the LPI and the simplified method using SPT and $V_s$.

## 3. Results and Discussion

The LPI was determined at 10 soil boring locations in West Tennessee for the peak ground acceleration (PGA) of 0.5g and the moment magnitude ($M_w$) of 7.5 using equations (1) and (8) for SPT data and equation (12) for $V_s$ data. According to the Memphis, Shelby County, Tennessee, Seismic Hazard Maps report of USGS (Cramer et al. 2004), the average PGA for 2% probability of exceedance in 50 years for this area is estimated to be 0.58±0.09g.

Table 2 provides a summary of the LPI results. Table 2 also includes the average FC of the soils encountered (16.5 % to 38%), the results of the comparison between the obtained LPIs of the two methods for each site are provided in Table 2. The comparison of obtained LPI using SPT- and $V_s$ -based methods show that for nine sites located in Quaternary Loess, Quaternary Alluvial, Cretaceous McNairy, and Tertiary, the $V_s$ method predicts different liquefaction potential than the SPT method and at only one site (Sommerville) both methods show the same LPI value of 0. It also can be observed that for seven sites the $V_s$-based method predicts a higher LPI value than the SPT-based method. The obtained LPI values from each of the methods are shown in Fig. 2, and it can be seen that generally, the $V_s$-based method gives a higher trend of LPI values than the SPT-based method. However, the differences between the two methods do not follow a consistent pattern range, and it varies from site to site [9-10, 14].

To check if there is a statistical relationship between two sets of LPI values of $V_s$ and SPT methods, a correlation coefficient between the results of the two methods was obtained using the following:

$$r = \frac{\sum(x_i - \bar{x})(y_i - \bar{y})}{\sqrt{\sum(x_i - \bar{x})^2 \sum(y_i - \bar{y})^2}} \quad (14)$$

where $r$ is the correlation coefficient, $x_i$ is values of $x$-variable in a sample (e.g., $V_s$-based LPIs), $\bar{x}$ is the mean of the values of the $x$ variable, $y_i$ is values of the $y$ variable (e.g., SPT-based LPIs), and $\bar{y}$ is the mean of the values of the $y$ variable.

From the correlation coefficient, the statistical consistency between two sets of LPI values was computed to be 0.29 in the range of [0,1], which is statistically interpreted as a weak correlation and shows that there is not a strong relationship between the two sets of LPI values.

**Table 2** Comparison of SPT- and $V_s$-based LPI values for 10 sites

| Site No. | Site name | Geology description | Avg. FC (%) | $V_s$-LPI | SPT-LPI |
|---|---|---|---|---|---|
| 1 | Route 14 | Quaternary Loess | 31 | 14 | 1 |
| 2 | Sommerville | Quaternary Loess | 16.5 | 0 | 0 |
| 3 | Covington | Quaternary Loess | 20 | 0 | 4 |
| 4 | Brownsville | Quaternary Loess | 38 | 0 | 9 |
| 5 | Newbern | Quaternary Loess | 23 | 27 | 0 |
| 6 | Trenton | Quaternary Loess | 25 | 26 | 11 |
| 7 | Wynnburg | Quaternary Alluvial | 18 | 9 | 2 |
| 8 | Selmer | Cretaceous McNairy | 36 | 24 | 11 |
| 9 | Jackson | Tertiary | 28 | 12 | 9 |
| 10 | Paris | Tertiary | 19 | 4 | 1 |

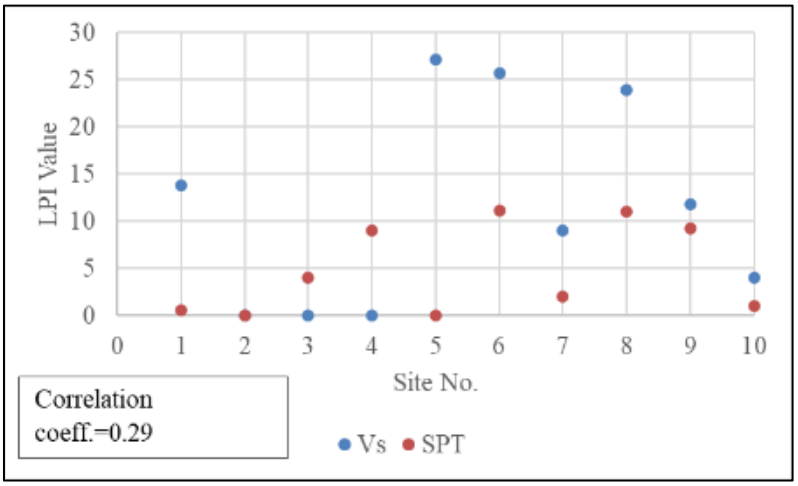


**Figure 2** $V_s$- and SPT-based LPI values

Additionally, a hypothesis test on the coefficient of correlation was done to check whether there is no correlation or some correlation between two sets of LPI values. The hypothesis test is defined in Table 3; a two tails hypothesis tests with a null and alternate hypothesis.

**Table 3** Conditions of the hypothesis test for this study

| | | |
|---|---|---|
| Null Hypothesis | $H_0: \rho = 0$ | No Correlation |
| Alternate Hypothesis | $H_1: \rho \neq 0$ | Some Correlation |

The next step with a hypothesis test is to find the p-value which describes how likely the null hypothesis is true, and it is the area under the standard normal distribution curve between the critical values of $t$ and -$t$ in two tails test. $t$ is calculated by equation 15.

$$t = \frac{r\sqrt{n-2}}{\sqrt{1-r^2}} \tag{15}$$

where $r$ is the correlation coefficient, and $n$ is the sample size. For this study, $t$ is equal to 14.638 which represents a statistically significant difference between calculated LPIs using SPT and $V_s$.

Once the *t*-value is calculated, using the TDIST function of Excel was utilized to compute the p-value and two tails distributions. For this study, the p-value is equal to *1.93856E-11,* which is much smaller than the significance level of 0.5, leading to rejecting the null hypothesis; therefore, evidence suggests some correlation between the two sets of LPI values.

As noted before, the primary differences in SPT- and $V_s$ - based methods of determining LPI are determination of CRR and the weighting function. For the SPT method, CRR is a function of $(N_1)_{60CS}$ and FC, and for the $V_s$ method, CRR is a function of $V_{s1}$ and FC. The parameter $w(z)$ is a function of the liquefiable layer depth. A liquefiable layer herein is defined as a layer that has three conditions:(1) the layer is saturated, (2) the layer's FC is less than 35%, and (3) $V_{s1}$ or $(N_1)_{60CS}$ value of below the upper limits of 210 m/s and 30, respectively.

The parameter FC is considered the same for both the SPT boring and $V_s$ profile obtained at the same site at each 1.4 m increment to a depth of 20 m. Also, the saturated layers of each site are the same for both SPT and $V_s$ profiles since the same GWL was utilized at each of the 10 locations for both SPT and $V_s$. Therefore, the upper limit values of $(N_1)_{60CS}$ and $V_{s1}$ is the condition that causes a difference in the number and the depth of liquefiable layers of the SPT and $V_s$ methods. The $V_{s1}$ value of layers at the upper limit value of $(N_1)_{60CS}$ (≥30) was extracted for all 10 sites. Fig. 3 illustrates that for 40% of layers at the upper limit of SPT *N*-value the $V_{s1}$ is not in agreement (it is not at the upper limit), and it is lower than 210 m/s which causes an increase in the number of liquefiable layers, and consequently a higher LPI for the $V_s$ method.

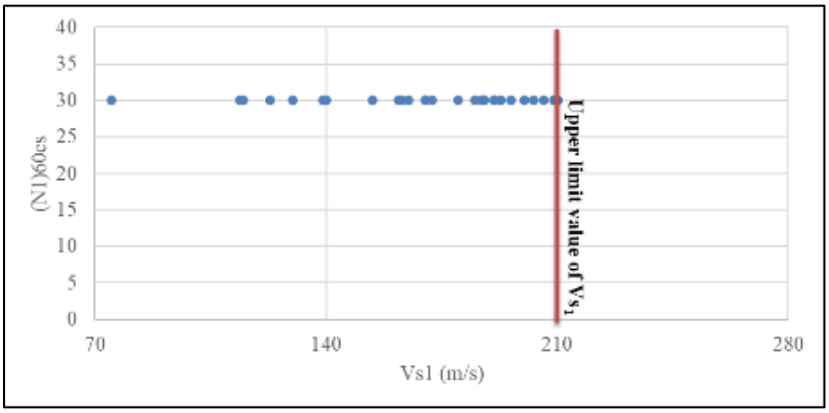


**Figure 3** $V_{s1}$ values at the layer with SPT N-values of 30 or more

Due to the inconsistency between upper limit values $V_{s1}$ and $(N_1)_{60CS}$, the number of liquefiable layers becomes different at each site following $V_s$ - and SPT-based methods. Therefore, the LPI values can be different between $V_s$ and SPT methods. Table 4 provides the number of liquefiable layers for each site based on $V_s$ and SPT methods. The number of liquefiable layers follows the trend of the LPI values provided in Table 4, which means that for the sites where $V_s$ shows a higher LPI value, the number of liquefiable layers based on the $V_s$ method is more than the SPT method and vice versa.

**Table 4** Comparison of SPT- and $V_s$-based LPI values for ten sites

| Site No. | Site name | Number of liquefiable layers based on $V_s$ method | Number of liquefiable layers based on SPT method |
|---|---|---|---|
| 1 | Route 14 | 6 | 3 |
| 2 | Sommerville | 0 | 0 |
| 3 | Covington | 0 | 1 |
| 4 | Brownsville | 0 | 7 |
| 5 | Newbern | 9 | 1 |
| 6 | Trenton | 5 | 2 |
| 7 | Wynnburg | 2 | 1 |

| | | | |
|---|---|---|---|
| 8 | Selmer | 5 | 2 |
| 9 | Jackson | 3 | 1 |
| 10 | Paris | 3 | 1 |

As provided in Table 4, for the majority of sites, the number of liquefiable layers at each site is different between $V_s$ and SPT procedures. Fig. 4 shows a comparison of the depth of liquefiable layers between $V_s$ and SPT methods for all 10 sites. As shown in Fig. 3, the depth of liquefiable layers varies between methods at each location. This discrepancy impacts the weighting function (10-0.5z) in equation (1), which decreases with an increase in depth. For example, for Jackson (site 9), both SPT and $V_s$ have three liquefiable layers, but the liquefiable layers are at different depths for each method. Therefore, weighting function values are different; consequently, different LPIs. The discrepancy between the number and depth of liquefiable layers contributes to the differences between SPT- and $V_s$ -based LPIs indicated in Fig. 4.

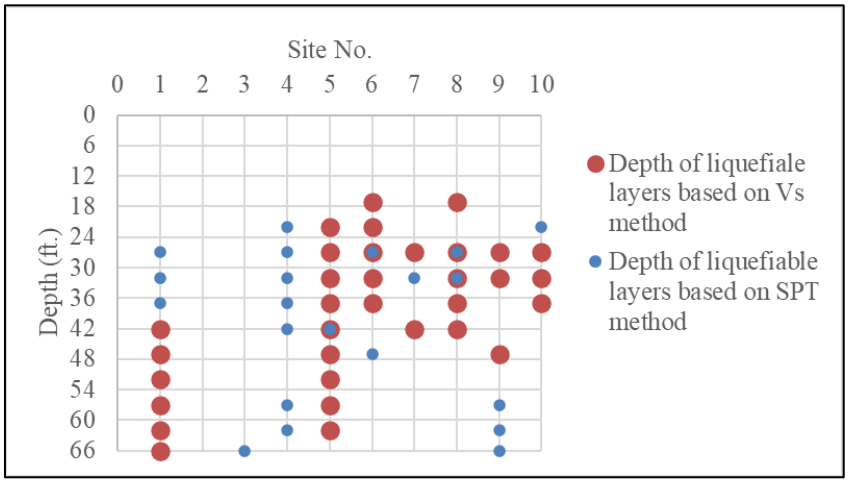


**Figure 4** Depth of liquefiable layers based on $V_s$ and SPT methods for each site

In addition to the differences in the weighting functions, the differences in CRR also contribute to differences in LPI between the $V_s$- and SPT-based methods. The difference between CRRs of each method causes the difference in FS and consequently LPIs. The differences in CRR are provided by the differences in the FC effect and by the variation in field $V_s$ and SPT values. As shown by equations (8) and (12), although the same FC was used for both $V_s$ and SPT methods of analysis for a specific site, the impact of FC on SPT-CRR (α and β) and $V_s$ -CRR (parameter $c$) may have unequal statistical effects on CRRs that needs to be evaluated using analytical tools. The statistical analysis is not addressed in this study.

The variation in field $V_s$ and SPT values is also a reason for the difference in CRRs of SPT and $V_s$ methods. For example, Kulhawy and Trautmann [28] suggest a coefficient of variation (COV) of 15-45% in field N values, and Toro et al. [29] suggest an approximate COV of 41% for $V_s$ values. EPRI [30] specifies a COV of 0.35 for profiles obtained using geotechnical site investigations and 0.50 for profiles inferred from obtained based on geology or topology. Also, the SPT hammer type, sampler type, rod length, and borehole diameter of SPT measurements were not available for the 10 sites. Thus, these corrections could not be applied, and $N_{60}$ was assumed to be equal to the field N.

Furthermore, according to a study done by Verdugo [19], it was concluded that $V_s$ is basically influenced by soil type, confining pressure, and soil density, but factors that have a high impact on liquefaction resistance such as over-consolidation and pre-shaking do not impact $V_s$, therefore, by using $V_s$ to compute CRR, the effect of OCR and pre-shaking have been not taken into analysis while the SPT N-value is significantly impacted by one the of the OCR functions which is the horizontal effective stress. Additionally, experimental work has found that $V_s$ cannot capture the relative density detail of soil layers, and it is known that the relative density is one of the parameters that significantly affect liquefaction potential analysis [19].

## 4. Conclusions

This study evaluated the liquefaction potential of soils using two in-situ test data, including SPT and $V_s$ following the general format of the simplified procedure of Seed and Idriss [1] presented by Youd-Idriss [17], and Andrus-Stokoe [26],

respectively. The comparison of liquefaction probability between the two methods for the study area revealed that for all four geology classifications of Quaternary Loess, Quaternary Alluvial, Cretaceous McNairy, and Tertiary with various averages of FC (16.5-38%), there is not an agreement between the SPT-based LPI and the $V_s$ -based LPI. The $V_s$-based simplified approach predicted a higher LPI than the SPT-based approach for seven sites, and it predicted a lower LPI than the SPT-based procedure for two sites; for only one site both methods predicted the same LPI value

The primary reasons for the differences in LPI values between $V_s$ - and SPT-based methods are the differences in the determination of CRR and the weighting function. One of the main reasons for differences in CRR and the weighting function is the inconsistency between the upper limit value of $V_{s1}$ and $(N_1)_{60CS}$. The inconsistency in the upper limit values of $V_s$ and $N$ causes the difference in the number and depth of liquefiable layers for each method. The discrepancy in the depth of the liquefiable layers through each method for the same location is the main reason for inconsistency in the weighting function between the two methods. It was found that for the sites where $V_s$ predicts higher LPI value, the $V_s$ also has more liquefiable layers than SPT method and the other way around. Besides, since the SPT-based CRR is a function of $(N_1)_{60CS}$, and the $V_s$ -based CRR is a function of $V_{s1,}$ the inconsistency between $V_{s1}$ and $(N_1)_{60CS}$ of liquefiable layer affects the CRR values of two methods; consequently FS, and LPI.

For future studies, the SPT and $V_s$ will be utilized to develop the liquefaction probability curves in order to assess the impact of the inconsistency between the two methods on liquefaction hazard maps of the West Tennessee area.

The findings of this study are limited to the analysis of 10 sites. Future research will include additional SPT and $V_s$ data (recorded at the same locations) from other sites in the Mississippi embayment and statistical analysis of SPT- and $V_s$-based CRR equations and variations of filed test measurements.

## Compliance with ethical standards

### *Disclosure of conflict of interest*

Hamed Tohidi declares no known competing financial interests or personal relationships that could have appeared to influence the work reported in this paper.

David Arellano declares no known competing financial interests or personal relationships that could have appeared to influence the work reported in this paper.

Shahram Pezeshk declares no known competing financial interests or personal relationships that could have appeared to influence the work reported in this paper.

## References

[1] Seed HB, Idriss IM. Simplified Procedure for Evaluating Soil Liquefaction Potential. Journal of the Soil Mechanics and Foundations Division., 1979;97(9):1249-1273. doi:10.1061/jsfeaq.0001662.

[2] Seed HB, and Idriss IM. Ground motions and soil liquefaction during earthquakes. Earthquake Engineering Research Institute Monograph, Oakland, Calif., 1982.

[3] Iwasaki T. A practical method for assessing soil liquefaction potential based on case studies at various sites in Japan. Second International Conference on Mierozonation for Safer Construction Research and Application, 1978.

[4] Iwasaki T, Arakawa T, Tokida K-I. Simplified procedures for assessing soil liquefaction during earthquakes. International Journal of Soil Dynamics and Earthquake Engineering. 1984;3(1):49-58. doi:10.1016/0261-7277(84)90027-5.

[5] Seed HB, Idriss IM, Arango I. Closure to evaluation of liquefaction potential using field performance data. Journal of Geotechnical Engineering 1985;111, 1346–1346.

[6] Robertson PK, Wride CEF. Evaluating cyclic liquefaction potential using the cone penetration test. Canadian Geotechnical Journal 1998;35, 442–459.

[7] Youd TL, Idriss IM. Liquefaction Resistance of Soils: Summary Report from the 1996 NCEER and 1998 NCEER/NSF Workshops on Evaluation of Liquefaction Resistance of Soils. Journal of Geotechnical and Geoenvironmental Engineering.2001;127(4):297-313. doi:10.1061/(ASCE)1090-0241(2001)127:4(297).

[8] Tohidi H., Arellano D., Cramer C.H. Initial liquefaction hazard mapping of Northwest Tennessee based on liquefaction probability curves. Geo-Extreme 2021.

[9] Chrisley J. Consistency between liquefaction prediction based on SPT, CPT, and VS measurements at the same sites (thesis)." Texas univ at Austin, United States., 2000.

[10] Juang CH, Jiang T., Andrus R.D. Assessing probability-based methods for liquefaction potential evaluation. Journal of Geotechnical and Geoenvironmental Engineering 2002;128, 580–589.

[11] Andrus RD, Piratheepan P, Ellis BS, Zhang J., Hsein Juang C. Comparing liquefaction evaluation methods using penetration-vs relationships. Soil Dynamics and Earthquake Engineering 2004;24, 713–721.

[12] Bradshaw AS., Baxter CD., Green RA. A site-specific comparison of simplified procedures for evaluating cyclic resistance of non-plastic silt. Dynamic Response and Soil Properties., 2007.

[13] Nasseri-Moghadam A., Provencal J., and Bennett J. Assessment of liquefaction potential at a site in Ottawa using SPT and shear wave velocities. 2011 Pan-Am CGS Geotechnical Conference.

[14] Khalil Noutash M., Dabiri R., and Hajialilue Bonab M. The Evaluation of Soil Liquefaction Potential Using Shear Wave Velocity Based on Empirical Relationships. International Journal of Engineering (IJE), 6(4)., 2012.

[15] Rollins K., Amoroso S., and Hryciw R. Comparison of DMT, CPT, SPT, and $V_s$ based Liquefaction Assessment on Treasure Island during the Loma Prieta Earthquake. 3rd International Conference on the Flat Dilatometer, 14-16 June 2015, Rome, Italy, 349–356.

[16] Rahmanian S., Rezaie F. Evaluation of liquefaction potential of soil using the shear wave velocity in Tehran, Iran." Geosciences Journal 2016;21, 81–92.

[17] Akkaya İ., Özvan A., Akin M., Akin M.K., Övün U. Comparison of SPT and V S-based liquefaction analyses: A case study in Erciş (Van, Turkey). Acta Geophysica 2017;66, 21–38.

[18] Oshnaviyeh D., and Dabiri R. Comparison of Standard Penetration Test (SPT) and Shear Wave Velocity ($V_s$) Methods in Determining Liquefaction Hazard along Tabriz Metro Line 2. Journal of Engineering Geology, 2018;12(2), 183–212.

[19] Verdugo R. Experimental and conceptual evidence about the limitations of shear wave velocity to predict liquefaction. Soil Dynamics and Earthquake Engineering 2016;91, 160–174.

[20] Pezeshk S., Camp C. V., Liu L., Evans J. M., and He J. Seismic Acceleration Coefficients for West Tennessee and Expanded Scope of Work for Seismic Acceleration Coefficients for West Tennessee Phase 2 - Field Investigation., 1998.

[21] Luna R., and Frost J. Spatial Liquefaction Analysis System. J. Comput. Civ. Eng., 1998;12(1), 48-56.

[22] Toprak S., Holzer T.L. Liquefaction potential index: Field assessment. Journal of Geotechnical and Geoenvironmental Engineering 2003;129, 315–322.

[23] Holzer T.L., Bennett M.J., Noce T.E., Padovani A.C., Tinsley J.C. Liquefaction hazard mapping with LPI in the Greater Oakland, California, area. Earthquake Spectra 2006;22, 693–708.

[24] Baise L. G., Higgins R. B., and Brankman C. M. Liquefaction hazard mapping Statistical and spatial characterization of susceptible units. J.Geotech.Geoenviron.Eng., 2006;132(6), 705-715.

[25] Idriss IM. An update to the Seed-Idriss simplified procedure for evaluating liquefaction potential. Proceedings. TRB Workshop on New Approaches to Liquefaction. 1999.

[26] Andrus RD, Stokoe II KH. Liquefaction resistance of soils from shear-wave velocity. Journal of Geotechnical and Geoenvironmental Engineering 2000;126, 1015–1025.

[27] Rix GJ. and Romero-Hudock S. Liquefaction potential mapping in Memphis and Shelby County, Tennessee, unpublished Rept. To the U.S. Geol. Surv., Denver Colorado, 27 pp., 2006.

[28] Kulhawy FH. and Trautmann CH. Estimation of in-situ test uncertainty. In C.D. Shackleford, P.P. Nelson and M.J.S. Roth (eds.), Uncertainty in the Geologic Environment: From Theory to Practice. Geotechnical Special Publication No. 58: 269-286. New York: ASCE, 1996.

[29] Toro G. Probabilistic models of site velocity profiles for generic and site-specific ground-motion amplification studies. Technical Rep, 779574, 1995.

[30] EPRI. Transmission Structure Foundation Design Guide, Electrical Power Research Institute. Report 1024138, 378 pp., 2012.